IEEE Open Access Journal of
Power and Energy

Received 29 March 2020; revised 27 July 2020 and 1 September 2020; accepted 3 October 2020. Date of publication 12 October 2020; date of current version 9 November 2020.

Digital Object Identifier 10.1109/OAJPE.2020.3030193

A Stochastic Two-Stage Model for the Integrated Scheduling of the Electric and Natural Gas Systems

NIKOLAOS G. KANELAKIS[1] (Graduate Student Member, IEEE), PANDELIS N. BISKAS[1] (Senior Member, IEEE), DIMITRIS I. CHATZIGIANNIS[2] (Member, IEEE), AND ANASTASIOS G. BAKIRTZIS[1] (Fellow, IEEE)

[1]Department of Electrical and Computer Engineering, Aristotle University of Thessaloniki, 54124 Thessaloniki, Greece
[2]Heron II Viotias S.A., 11526 Athens, Greece

CORRESPONDING AUTHOR: P. BISKAS (pbiskas@auth.gr)

ABSTRACT The inherent coupling of the electric and natural gas systems due to the operation of gas generating units and power-to-gas facilities, along with the uncertainties faced in both systems due to the variability in electricity and gas demand and the vastly increasing volatile renewable injections, create an imperative need to schedule and operate the two systems in a coordinated manner. In this paper a new model for the fully integrated stochastic day-ahead scheduling of electric and gas systems is presented, coping with the uncertainties of both systems. The stochastic parameters comprise the electricity demand and the renewable injections, which collectively create several net electricity load scenarios, and the gas residential/industrial demand. The integrated scheduling problem concerns a unit commitment for the electricity problem, amended with additional constraints imposed by the underlying natural gas transmission system considering steady-state flow. A two-stage stochastic programming model is devised, having as second stage the possible realizations of net electricity load and gas demand in real-time. The model is tested in medium-size real-world test systems – the Greek electricity and gas systems – deriving useful insights on the advantages of the integrated stochastic scheduling versus the deterministic scheduling of the electricity and gas systems.

INDEX TERMS Electricity system, natural gas system, integrated scheduling, mixed integer linear programming, two-stage stochastic programming.

I. NOMENCLATURE

A. INDICES AND SETS

$a \in \mathcal{A}$	Set of gas network arcs $a = (m, n) \in \mathcal{A}$, where $\mathcal{A}_{pi} \subseteq \mathcal{A}$ is the subset of passive arcs, $\mathcal{A}_{act}$ the subset of active arcs, $\mathcal{A}_{cm}$ the subset of active arcs with compressors and $\mathcal{A}_{cv}$ the subset of active arcs with control valves; $\mathcal{A}_{cm} \cup \mathcal{A}_{cv} = \mathcal{A}_{act} \subseteq \mathcal{A}$
$b \in \mathcal{B}$	Set of steps of generating units' priced energy offers
$g \in \mathcal{G}$	Set of generating units, where $\mathcal{G}^{thr}$ is the subset of thermal units, $\mathcal{G}^{hdr}$ the subset of hydro units and $\mathcal{G}^{gas}$ is the subset of gas-fired generating units; $\mathcal{G}^{gas} \subseteq \mathcal{G}^{thr}$
$r \in \mathcal{R}$	Set of available reserve types; *res = {1: Frequency Containment Reserve (FCR), 2up: automatic Frequency Restoration Reserve (aFRR) up, 2dn: aFRR down, 3: manual Frequency Restoration Reserve(mFRR)}*
$d \in \mathcal{D}$	Set of directions (up / down) for reserve provision
$m \in \mathcal{V}$	set of gas nodes where $\mathcal{V}_{en} \subseteq \mathcal{V}$ is the subset of entry nodes, $\mathcal{V}_{ex} \subseteq \mathcal{V}$ the subset of exit nodes, $\mathcal{V}_{en}$ the subset of non-electric exit nodes and $\mathcal{V}_e$ the subset of electric exit nodes; $\mathcal{V}_{ne} \cup \mathcal{V}_e = \mathcal{V}_{ex} \subseteq \mathcal{V}$
$s \in \mathcal{S}$	Set of scenarios
$t \in \mathcal{T}$	Set of scheduling/dispatch periods (in hours)
$x \in \mathcal{X}$	Set of bidding areas in the power system

B. PARAMETERS

P^b_{gt}/EQ^b_{gt}	Price / quantity pair of step b of the energy offer of gen. unit g in trading period t, in (€ /MWh, MWh)
P^r_{gt}	Price of the reserve offer for the provision of reserve type r of gen. unit g in trading period t, in € /MW/h
SUC_g/SDC_g	Generating unit g start-up/shut-down costs, in €
Q^{imp}_t/Q^{exp}_t	Total imports / exports in trading period t, in MWh
E^{max}_g/E^{min}_g	Maximum / minimum technical power output of generating unit g, in MW
E^{mand}_{gt}	Mandatory injection of hydro generating unit or generating unit under commision g in trading period t, in MW
RU_g/RD_g	Maximum ramp-up / ramp-down rates of generating unit g, in MW/min
UT_g/DT_g	Minimum up / down time of generating unit g, in hours
D_{xts}	Electricity load forecast in bidding area x in trading period t and scenario s, in MWh
$FL^{\max}_{xx't}$	Maximum flow in the corridor between bidding areas x and x' in trading period t, in MW
R^r_g	Maximum technical capability of generating unit g to provide reserve type r, in MW
RR^r_t	System reserve requirement for reserve type r in trading period t, in MW
a_g, b_g, c_g	Gas-fired generating unit $g \in \mathcal{G}^{gas}$ fuel consumption coefficients, in GJ, GJ/MWh and GJ/MW^{2}h, respectively
c_a	Compressor operation cost, in € /kW/h
γ	Non-electric gas demand shedding cost, in € /Nm^3/h
d^m_{ts}	Non-electric gas demand target at outgoing node $m \in \mathcal{V}_{ex}$ in trading period t and scenario s, in Nm^3/h
$\underline{p^m}/\overline{p^m}$	Min/Max pressure technical bounds of gas node m at arc $m \in \mathcal{V}$, in bar
$\underline{q^a}/\overline{q^a}$	Min/Max gas flow bounds through gas node $a \in \mathcal{A}$, in Nm^3/h
η_a	Adiabatic efficiency of compressor at active arc $a \in \mathcal{A}_{cm}$
$\underline{HP^a}/\overline{HP^a}$	Min/Max horsepower technical bounds of compressor at active arc $a \in \mathcal{A}_{cm}$, in MW
$\underline{rt^a}/\overline{rt^a}$	Min/Max pressure ratio bounds of compressor at active arc $a \in \mathcal{A}_{cm}$
$\underline{\Delta^a}/\overline{\Delta^a}$	Min / Max pressure decrease bounds of control valve at active arc $a \in \mathcal{A}_{cv}$, in bar
L_α/D_α	Length and diameter and cross-sectional area of $a \in \mathcal{A}$, in m
$\mathcal{A}_\alpha$	Cross-sectional area of pipeline $a \in \mathcal{A}$, in m^2
λ_α	pipeline roughness of $a \in \mathcal{A}$, in m
z	Mean Compressibility factor
$\mathcal{T}$	Mean temperature, in K
R_s	Universal gas constant, in J/mol K
k	Gas constant isentropic exponent
H	Higher Heating Value of natural gas, in GJ/Nm^3
π_s	Realization probability for scenario s, in %

C. MAIN VARIABLES

u_{gts}/u^{AGC}_{gts}	Binary variable denoting that generating unit g is committed / in AGC mode during trading period t and scenario s, if equal to 1
w_{gt}	Binary scenario-independent variable associated with u_{gts}/u^{AGC}_{gts}, denoting the commitment status of thermal unit g during time period t
y_{gts}/z_{gts}	Binary variable denoting that thermal unit g starts-up / shuts-down during trading period t and scenario s, if equal to 1
v_{gt}/ζ_{gt}	Binary scenario-independent variables associated with y_{gts}/z_{gts}, denoting the start-up/shut-down status of thermal units g during time period t
i^α_{ts}	Binary variable denoting the operational state of compressor $a \in \mathcal{A}_{cm}$ during trading period t and scenario s; active if equal to 1, closed if equal to 0
ib^α_{ts}	Binary variable denoting the operational state of parallel bypass valve at active arc $a \in \mathcal{A}_{cm}$ during trading period t and scenario s; open if equal to 1, closed if equal to 0
h^α_t	Binary scenario-independent variable associated with i^α_{ts}, denoting the operational status of compressor $a \in \mathcal{A}_{cm}$ during trading period t
j^α_{ts}	Binary variable denoting the operational state of control valve $a \in \mathcal{A}_{cv}$ during trading period t and scenario s; active if equal to 1, closed if equal to 0
ξ^α_t	Binary scenario-independent variable associated with j^α_{ts}, denoting the operational status of control valve $a \in \mathcal{A}_{cv}$ during trading period t
e_{gts}	Cleared energy production of generating unit g in trading period t and scenario s, in MWh
eq^b_{gts}	Cleared quantity of step b of generating unit g energy offer in trading period t and scenario s, in MWh
r^r_{gts}	Reserve award for reserve type r by generating unit g in trading period t and scenario s, in MW
$fl_{xx'ts}$	Electricity flow between bidding areas x and x' in trading period t and scenario s, in MWh/h
p^m_{ts}	Node pressure at node m in trading period t and scenario s, in bar
q^a_{ts}	Gas flow through arc $a \in \mathcal{A}$ in trading period t and scenario s, in Nm^3/h

s_{ts}^{m} Curtailed residential/industrial gas demand at outgoing node $m \in \mathcal{V}_{ex}$ in trading period t and scenario s, in Nm^3/h

HP_{ts}^{a} Horsepower of compressor at active arc $a \in \mathcal{A}_{cm}$ in trading period t and scenario s, in kW

II. INTRODUCTION

THE interdependency of the power system and the natural gas network has been highlighted by the research community and practitioners in the last ten years [1]–[3]. Such interdependency stems mainly from the increased utilization of flexible / fast-response gas-fired power units in the electricity production portfolio, (a) used to offset the variations of the vastly increasing renewable injections, and (b) following global environmental concerns leading to politically-driven binding decarbonization targets, and to less extent from power-to-gas (P2G) facilities. This interdependency is expressed in many ways; indicatively we refer to (a) the gas network pressure and flow constraints that affect the commitment and scheduling of gas power units, (b) the effect of gas transportation cost on the overall variable cost of gas power units and consequently on their competitiveness in the wholesale electricity market, (c) the effect of gas storage facilities on handling the variability and uncertainty introduced by the renewable injections and on the security of supply of the power system, (d) the effect that contingencies on the electricity grid have on the pressures and flows at the gas network, and inversely (e) the effect of gas network contingencies on the commitment and scheduling of gas power units when covering the electricity load and the system reserve requirements. The increasing interdependency between the two energy systems are expected to lead to even tighter coordinated -or even integrated- scheduling and operation approaches.

In the literature there is a clear differentiation between:

(a) the coordinated operation of the power and gas systems [4]–[8], namely the separate scheduling and operation of each system, but with a -usually iterative- coordination process during which the technical infeasibilities of one problem are passed as binding constraints to the other problem until all infeasibilities are gradually resolved at the end of the coordination process, and

(2) the integrated co-optimization (scheduling and operation) of the two systems [9]–[14], namely the solution of a single problem targeting at the minimization of the overall cost of both systems, respecting the technical constraints of both systems, and being solved at one-shot for the optimal combined solution.

Apparently, the theoretically optimal solution is the second one, leading to the overall optimal solution. Further differentiation in such problems concerns the consideration of the steady-state or transient gas flows, and the deterministic or stochastic formulation of the coordinated/integrated scheduling problems.

There is a rich literature on deterministic formulations [4]–[14]; an extensive and thorough discussion on recent research works is provided in [15]. Recently, more sophisticated approaches have been presented with novel linearization algorithms, as per second order cone relaxations in [8] and [14]. However, the deterministic approaches may fail to incorporate the inherent stochasticity of several parameters affecting the day-ahead power and gas scheduling solution, such as the level of the electricity load, the renewable injections (especially of wind and PV stations) and the gas load from residential, commercial and industrial consumers. On the contrary the stochastic formulation of the integrated problem is able to provide a solution that considers a large set of probable realizations of the stochastic parameters in real-time (based on respective realization probabilities).

Several stochastic formulations for the efficient operation of power systems under high renewable generation have been presented in the last years [16]. The application of stochastic methodologies on the common scheduling problem of electricity and gas systems has been studied during the last years due to their increasing interdependence. The majority of the relevant literature relies on two-stage stochastic formulations that calculate optimal commitment schedules for generating units and gas wells under several stochastic parameters. In [17] the authors examine the effects of contingencies on the day-ahead scheduling using mixed-integer relaxation of the gas constraints. The effect of uncertainty in gas supply is also examined in [18], where a two-stage coordination algorithm on a simplified Great Britain network is applied to evaluate the significant change in costs and energy reallocation that supply disruptions cause on the electricity scheduling. The same network is also utilized by Qadrdan et al in [19] under two- and multi-stage formulations that demonstrate the effectiveness of stochastic consideration of wind uncertainty in terms of operational cost savings. Authors in [20] address the wind uncertainty by considering the use of energy storage applications in multi-objective market clearing, whereas [21] offers a clear comparison of scheduling under wind uncertainty between deterministic and stochastic approaches to demonstrate the economic effectiveness of the latter. In [22] the authors execute a stochastic SCUC considering component outages and load forecasting errors in an iterative procedure with natural gas network feasibility subproblems.

Reference [23] extends the stochastic consideration of energy systems in a micro-grid level where operational and environmental objectives are optimized against various stochastic parameters exploiting the P2G concept. In [24], Zhao *et al.* formulated a two-stage stochastic approach where the operational costs of gas-fired units are optimized by considering uncertainty on fuel price and scarcity. In [25] the authors presented a multi-stage stochastic framework with adaptive refinements and a thorough modeling of the configurations and transitions of combined-cycle units, which led to better operational utilization of the gas network.

The uncertainty consideration in the form of robust programming implementations has also gained traction recently in the literature [26]–[28], where the integrated optimization problem is optimized over the worst-case situation based on a predefined uncertainty set. In [26] the authors propose a robust formulation for wind power uncertainty to ensure that the system can sustain N–1 contingency events of transmission line and gas pipeline loss. A decomposition-based approach is adopted in [27] to iteratively solve the long-term co-planning problem; the method optimizes base-case operational decisions in a master problem and checks the solution quality of the master problem via N-1 and probabilistic reliability criteria in two subproblems that identify the worst-case realizations. A two-stage robust problem is presented in [28], which is decomposed by second-order cone-based column and constraint generation into the first-stage base case operation master problem and gas security-check subproblems, highlighting the gas-side contribution in system efficiency enhancement. Additional applications of robust optimization framework have been proposed in [29] and [30], where second-order cone programming is applied to address various uncertainties and contingencies for day-ahead energy and reserve scheduling. The authors in [29] consider a two-stage adaptive model which is in turn converted and solved via a novel iterative algorithm which reduces the number of scenarios, while in [30] energy and reserves are scheduled against load and renewable uncertainty with SOC-based relaxation of nonconvexities is followed by gas-flow corrections in order to avoid sequential, less efficient solutions.

A new approach for dealing with uncertainties in the integrated power-gas system has also been proposed in the form of distributionally robust optimization, where the system is optimized considering worst-case probability distributions as ambiguity sets with partial distributional information. In [31] a two-stage formulation for calculation of locational prices under demand response from both systems is implemented, while in [32] the integrated system is optimized under wind uncertainty.

Overall, the basic features of each stochastic power-gas research work along with the respective features in this paper are summarized in Table 1.

All relative works have presented results that, while considering different gas network configurations and various gas-side stochastic variable realizations, utilized the gas network mainly to schedule the power network in a more reliable and robust way, without consideration for gas network scheduling decisions. Additionally, even though the considered gas networks range from small single-node systems to real-world systems, they are generally modelled without increased attention to precise parameterization that could considerably alter the attained results. In this paper, the authors present a two-stage stochastic optimization problem with uncertainty on both the electricity and the gas side, that incorporates (a) the full unit-commitment modeling for the explicit modeling of the electricity power system and (b) a detailed configuration of the gas network incorporating linearized gas network constraints. The main contributions of this paper are the following:

a) the incorporation of the detailed gas flow modeling with three distinct linearization techniques (extended incremental method, outer approximation method, big-M method) for the linearization of the Weymouth equation, the compressor flow equation and the electricity/gas coupling equation, respectively,
b) the consideration of binding scheduling decisions of the active, controllable gas network components (compressors, control valves) in the first stage (i.e. day-ahead scheduling phase) regarding their configuration/operation mode, which provides an operating schedule to be followed at the second stage (i.e. real-time dispatch phase), as well as the assessment of such biding scheduling decisions in the real-time gas network operation,
c) the evaluation of the stochastic programming model in a medium-size real-world test system.

The remaining of the paper is organized as follows: Section III presents the analytical formulation of the proposed novel two-stage stochastic mathematical problem. Section IV presents the computational results of the model application in a real-world test case system. Finally, Section V quotes the basic conclusions and findings of the conducted research.

III. MATHEMATICAL FORMULATION

The following section presents the mathematical formulation of the proposed stochastic integrated approach.

A. OBJECTIVE FUNCTION

The objective function is formulated as follows:

$$Min \sum_{s\in\mathcal{S}} \pi_s \left[C_s^{EL} + C_s^{GAS} \right] \tag{1}$$

where

$$C_s^{EL} = \sum_t \left[\sum_g \begin{bmatrix} P_{gt}^b \cdot eq_{gts}^b + \sum_r P_{gt}^r \cdot r_{gts}^r \\ +SUC_g \cdot y_{gts} + SDC_g \cdot z_{gts} \end{bmatrix} \right] \quad \forall s \in \mathcal{S} \tag{2}$$

$$C_s^{GAS} = C_s^{CM} + C_s^{SH} \quad \forall s \in \mathcal{S} \tag{3}$$

$$C_s^{CM} = \sum_{t\in\mathcal{T}} \left[\sum_{a\in A_{cm}} \left[c_a \cdot P_{ts}^a \right] \right] \quad \forall s \in \mathcal{S} \tag{4}$$

$$C_s^{SH} = \sum_{t\in\mathcal{T}} \left[\sum_{m\in V_{ne}} \left[\gamma \cdot s_{ts}^m \right] \right] \quad \forall s \in \mathcal{S} \tag{5}$$

The two terms of the objective function represent the costs of the electricity and the gas systems; the electricity system cost comprises the offer-based generation cost for energy production and reserve provision plus the start-up and shut-down costs, whereas the gas system cost comprises the compressor cost (cost of operating the compressor at a certain mechanical

TABLE 1. Relevant features of stochastic programming and robust optimization works reported in the literature.

No.	Solution methodology	Gas network flows representation	No. of stages	Stochastic parameters	1st stage decisions	2nd stage decisions	No. of scenarios in 2nd stage	Compressor formulation / decision variable	Test case(s)
[17]	integrated co-optimization	steady-state	two-stage	outages of pipelines and transmission lines	schedule of generating units, gas storage and gas wells	dispatching corrections in 1st stage decisions	3	simplified linear formulation, no use of binary variables	IEEE 24-bus power system and 20-node Belgian gas network
[18]	coordinated scheduling	transient-state	two-stage	gas and electric load demand, wind production and gas supply outages	commitment decisions, power and reserve scheduling	RES and load curtailments	9	simplified linear formulation, no use of binary variables	simplified electricity and gas networks for GB
[19]	integrated co-optimization	transient-state	two-stage and multi-stage	Wind power forecast	unit-commitment decisions	energy and reserve redispatching	5	detailed formulation, no use of binary variables	simplified electricity and gas networks for GB
[20]	integrated co-optimization	steady-state	two-stage	electric & gas load and wind production	schedule of generating units, compressed air energy storage, reserve awards	dispatching corrections in 1st stage decisions	10	simplified linear formulation, no use of binary variables	IEEE 24-bus system + 10-node gas system
[21]	integrated co-optimization	steady-state	two-stage	wind power forecast	binary unit commitment decisions, gas supply	dispatching corrections in 1st stage decisions	27	simplified linear formulation, no use of binary variables	IEEE 24-bus system with a 20-node gas system
[22]	coordinated scheduling	steady-state	two-stage	outages of generating units and transmission lines and electricity load	unit-commitment decisions	energy scheduling	4	simplified linear formulation, no use of binary variables	IEEE 118–bus power system with a ten-node gas transmission network.
[23]	coordinated scheduling	steady-state	two-stage	loads for electricity, heat, and natural gas supplies, as well as the variability of WT and solar PV energy supplies	schedule of electricity and gas resources	dispatching corrections in 1st stage decisions	11	no compressor simulation, no use of binary variables	test microgrid
[24]	integrated scheduling	-	two-stage	gas fuel price and availability	unit commitment decisions	dispatching corrections in 1st stage decisions	up to 10	-	8-zone test system and 240-node system
[25]	integrated scheduling	steady-state	multi-stage	electricity load demand and wind power output	unit-commitment and CCGT transition decisions	power generation and gas dispatch	up to 200	simplified linear model	IEEE 24-bus-20-node system
[28]	integrated scheduling	steady-state	two-stage	transmission lines outage events	power and gas commitment and generation scheduling	unit redispatch, gas generation adjustments, corrective power shedding	uncertainty set of N-k criteria	-	a 6-bus-6-node and IEEE 118-bus-10-node IEGS
[29]	integrated scheduling	steady-state	two-stage	RES generation	energy and reserve dispatch	energy redispatch and load shedding balancing	up to 50	simplified linear	Coupled 13-node electricity and 9-node gas urban networks
[30]	integrated scheduling	steady-state	-	electricity load and renewable generation	energy and reserve dispatch	-	uncertainty forecast errors interval	linear simplification of higher-order compressor consumption	IEEE 39-bus-15-node and 118-bus-40-node test IEGS
This paper	integrated co-optimization	steady-state	two-stage	electricity net load, gas load	commitment of generating units, commitment of gas compressor	energy and reserve schedules of generating units, compression rate of compressor	9	detailed formulation of compressor operation with binary variables	Greek power system and the 89-node Greek gas system

power level) and the gas shedding cost (cost incurred in case of residential/industrial gas load curtailment).

B. ELECTRICITY SYSTEM CONSTRAINTS

The electricity subproblem is presented in this section; the following equations express the system and unit operating constraints.

$$\sum_{g\in\mathcal{G}_x} e_{gts} + Q_t^{imp} - D_{xts} - Q_t^{\exp} = \sum_{x'\in\mathcal{X}} (fl_{xx'ts} - fl_{x'xts}) \quad \forall x \in \mathcal{X}, t \in \mathcal{T}, s \in \mathcal{S} \qquad (6)$$

$$fl_{xx'ts} \leq FL^{max}_{xx't} \quad \forall x, x' \in \mathcal{X}, t \in \mathcal{T}, s \in \mathcal{S} \tag{7}$$

$$\sum_{g \in \mathcal{G}} r^{rd}_{gts} \geq RR^{rd}_{t} \quad \forall d \in \mathcal{D}, r \in \mathcal{R}, \forall t \in \mathcal{T}, s \in \mathcal{S} \tag{8}$$

Equation (6) denotes the area power balance constraint, constraint (7) limits the energy exchange between two neighboring bidding areas to the respective corridor flow limit, whereas equations (8) denote the system-wide reserve requirements for primary, secondary up & down and tertiary reserve that should be covered from the generating units.

$$y_{gts} + z_{gts} \leq 1 \quad \forall g \in \mathcal{G}, \quad t \in \mathcal{T}, \ s \in \mathcal{S} \tag{9}$$

$$y_{gts} - z_{gts} = u_{gts} - u_{g,t-1,s} \quad \forall g \in \mathcal{G}, \ t \in \mathcal{T}, s \in \mathcal{S} \tag{10}$$

$$u^{AGC}_{gts} \leq u_{gts} \quad \forall g \in \mathcal{G}, \quad t \in \mathcal{T}, \ s \in \mathcal{S} \tag{11}$$

$$\sum_{\tau=t-UT_g+1}^{\tau=t} y_{gts} \leq u_{gts} \quad \forall g \in \mathcal{G}^{thr}, \ t \in \mathcal{T}, s \in \mathcal{S} \tag{12}$$

$$\sum_{\tau=t-DT_g+1}^{\tau=t} z_{gts} \leq 1 - u_{gts} \quad \forall g \in \mathcal{G}^{thr}, \ t \in \mathcal{T}, s \in \mathcal{S} \tag{13}$$

Constraints (9)-(13) denote the logical relationship between binary variables u_{gts}, u^{AGC}_{gts}, y_{gts} and z_{gts}. Equation (9) forces that a generating unit may not simultaneously start-up and shut-down at the same trading period, whereas equation (10) ensures the continuous operation of generating unit g, between its synchronization and its shut-down. Constraint (11) allows generating unit g to enter in its AGC mode only if it is committed. Finally, equations (12) and (13) enforce minimum up and down limits to thermal generators' operation; it is assumed that hydro generating unit have the capability to start-up and shut-down within one hour; thus, such constraints are deemed unnecessary.

$$e_{gts} - e_{g,t-1,s} \leq 60 \cdot RU_g \cdot \left(u_{gts} - u^{AGC}_{gts}\right) + 60 \cdot RU^{AGC}_{g} \cdot u^{AGC}_{gts} + M^{U} \cdot y_{gts} \quad \forall g \in \mathcal{G}^{thr}, \quad t \in \mathcal{T}, \ s \in \mathcal{S} \tag{14}$$

$$e_{g,t-1,s} - e_{gts} \leq 60 \cdot RD_g \cdot \left(u_{gts} - u^{AGC}_{gts}\right) + 60 \cdot RD^{AGC}_{g} \cdot u^{AGC}_{gts} + M^{D} \cdot z_{gts} \quad \forall g \in \mathcal{G}^{thr}, \quad t \in \mathcal{T}, \ s \in \mathcal{S} \tag{15}$$

Equations (14) and (15) denote the ramp-up and ramp-down limitations of thermal generating units. Big M values M^U and M^D are used for the deactivation of the aforementioned constraints, during the start-up and shut-down procedures. It is assumed that hydro units exhibit increased flexibility, being able to reach their maximum capacity within one hour; thus, no ramping constraints are required for hydro units.

$$r^{FCR}_{gts} \leq R^{FCR}_{g} \cdot u_{gts} \quad \forall g \in \mathcal{G}^{thr}, \ t \in \mathcal{T}, s \in \mathcal{S} \tag{16}$$

$$r^{aFRRup}_{gts} + r^{aFRRdn}_{gts} \leq R^{aFRR}_{g} \cdot u^{AGC}_{gts} \quad \forall g \in \mathcal{G}^{thr}, \ t \in \mathcal{T}, s \in \mathcal{S} \tag{17}$$

$$r^{mFRR}_{gts} \leq R^{mFRR}_{g} \cdot u_{gts} \quad \forall g \in \mathcal{G}^{thr}, \ t \in \mathcal{T}, s \in \mathcal{S} \tag{18}$$

$$r^{FCR}_{gts} \leq R^{FCR}_{g} \quad \forall g \in \mathcal{G}^{hdr}, \ t \in \mathcal{T}, s \in \mathcal{S} \tag{19}$$

$$r^{aFRRup}_{gts} + r^{aFRRdn}_{gts} \leq R^{aFRR}_{g} \quad \forall g \in \mathcal{G}^{hdr}, \ t \in \mathcal{T}, s \in \mathcal{S} \tag{20}$$

$$r^{mFRR}_{gts} \leq R^{mFRR}_{g} \cdot u_{gts} \quad \forall g \in \mathcal{G}^{thr}, \ t \in \mathcal{T}, s \in \mathcal{S} \tag{21}$$

Constraints (16)-(21) enforce upper limits to the provision of primary, secondary and tertiary reserve by thermal and hydro generating units.

$$e_{gts} = E^{mand}_{gt} + \sum_{b \in B} eq^{b}_{gts} \quad \forall g \in \mathcal{G}, \ t \in \mathcal{T}, s \in \mathcal{S} \tag{22}$$

$$eq^{b}_{gts} \leq EQ^{b}_{gt} \quad \forall g \in \mathcal{G}, \ t \in \mathcal{T}, s \in \mathcal{S} \tag{23}$$

$$e_{gts} - r^{aFRRdn}_{gts} \geq E^{min}_{g} \cdot \left(u_{gts} - u^{AGC}_{gts}\right) + E^{min,AGC}_{g} \cdot u^{AGC}_{gts} \quad \forall g \in \mathcal{G}^{thr}, \quad t \in \mathcal{T}, \ s \in \mathcal{S} \tag{24}$$

$$e_{gts} + r^{aFRRup}_{gts} \leq E^{max}_{g} \cdot \left(u_{gts} - u^{AGC}_{gts}\right) + E^{max,AGC}_{g} \cdot u^{AGC}_{gts} \quad \forall g \in \mathcal{G}^{thr}, \quad t \in \mathcal{T}, \ s \in \mathcal{S} \tag{25}$$

$$e_{gts} + r^{FCRup}_{gts} + r^{aFRRup}_{gts} + r^{mFRRup}_{gts} \leq E^{max}_{g} \cdot u_{gts} \quad \forall g \in \mathcal{G}, \quad t \in \mathcal{T}, \ s \in \mathcal{S} \tag{26}$$

$$e_{gts} - r^{aFRRdn}_{gts} \geq 0 \quad \forall g \in \mathcal{G}^{hdr}, \ t \in \mathcal{T}, s \in \mathcal{S} \tag{27}$$

Generating units' power output is limited by equations (22)-(27). Unit output is equal to a mandatory component (depicting either the unit commissioning-related generating profile or mandatory hydro injection) and the cleared part of the respective priced energy offer (the clearing quantity is limited by the submitted priced energy offer – eq. (23)). Equations (24)-(27) express that the total power output along with the reserve contribution should be limited by the technical characteristics of the examined generating unit. In general, thermal generating units have different minimum and maximum capacity limits when they operate in AGC mode, whereas the technical minimum of hydro units was taken equal to zero.

C. GAS SYSTEM CONSTRAINTS

The modeling of gas transportation networks refers to the set of partial differential equations that govern the physics of spatio-temporal relations between gas flows and pressures. The formulation of gas network in this paper follows the analytical description presented in [33] and [35], where the network is described by means of a directed finite graph $\mathcal{G} = (\mathcal{V}, \mathcal{A})$ of a set of nodes $m, n \in \mathcal{V}$ and arcs $a = (m, n) \in \mathcal{A}$. The node set $\mathcal{V}$ is further partitioned into gas injection nodes $\mathcal{V}_{en}$ and gas withdrawal nodes $\mathcal{V}_{ex}$, which in turn are denoted according to the load distinction as electric gas loads $\mathcal{V}_{e}$, corresponding to gas consumption of gas-fired generating units, and non-electric gas loads $\mathcal{V}_{ne}$, corresponding to gas consumptions of residential, commercial and industrial loads. Arc set $\mathcal{A}$ is partitioned into passive pipes set $\mathcal{A}_{pi}$ and active set

$\mathcal{A}_{act}$, further denoted as either compressor set $\mathcal{A}_{cm}$ or control valve set $\mathcal{A}_{cv}$. Positive pressure and free flow variables are associated with nodes and arcs, respectively, and are both bounded by technical upper and lower limits, as per (28)-(29).

$$\underline{p^m} \leq p^m_{ts} \leq \overline{p^m} \quad \forall m \in \mathcal{V}, t \in \mathcal{T}, s \in \mathcal{S} \tag{28}$$

$$\underline{q^a} \leq q^a_{ts} \leq \overline{q^a} \quad \forall a \in \mathcal{A},\ t \in \mathcal{T}, s \in \mathcal{S} \tag{29}$$

Nodal balance dictates that gas mass flow is conserved through every node m:

$$\sum_{a \in \delta^{in}(m)} q^a_{ts} - \sum_{a \in \delta^{out}(m)} q^a_{ts} = q^m_{ts} \quad \forall m \in \mathcal{V},\ t \in \mathcal{T}, s \in \mathcal{S} \tag{30}$$

where $\delta^{in}(m)$ and $\delta^{out}(m)$ denote the ingoing and outgoing arcs for every node m.

In order to ensure pressure feasibility, withdrawal target d^m_{ts} is relaxed via a shedding term s^m_{ts}, such that:

$$q^m_{ts} + s^m_{ts} = d^m_{ts} \quad \forall m \in \mathcal{V}_{ex},\ t \in \mathcal{T}, s \in \mathcal{S} \tag{31}$$

Assuming isothermal conditions, pressure decrease along a passive pipe is calculated by the well-established Weymouth equation:

$$p^{m2}_{ts} - p^{n2}_{ts} =, \frac{L_a \cdot \lambda_\alpha \cdot R_s \cdot z \cdot \mathcal{T}}{A^2_a \cdot D_a} \cdot |q^a_{ts}| \cdot q^a_{ts} \quad \forall a \in \mathcal{A}_{pi}, \quad t \in \mathcal{T}, s \in \mathcal{S} \tag{32}$$

where the mean temperature T is equal to 289.15 K, the pipeline roughness λ_α equal to 0.00810e^{-3} and the average compressibility factor z equal to 0.9.

In order to compensate pressure decrease over long distances, compressor machines are utilized to provide pressure boost. Their operating range is defined by its characteristic diagram, which is given by a set of curves obtained by (bi)quadratic least squares fits from measured data points that are expressed as nonlinear inequalities in the form of:

$$f(q^a, H^a_{ad}) \leq 0 \quad \forall a \in \mathcal{A}_{cm} \tag{33}$$

Typically, compressors constitute mechanical machines whose power consumption HP^a_{ts} is calculated as follows:

$$HP^a_{ts} = \frac{q^a_{ts} \cdot R_s \cdot \mathcal{T} \cdot z}{\eta_a} \cdot \frac{k}{k-1} \cdot \left[\left(\frac{p^n_{ts}}{p^m_{ts}}\right)^{\frac{k-1}{k}} - 1\right] \quad \forall a \in \mathcal{A}_{cm}, \quad t \in \mathcal{T},\ s \in \mathcal{S} \tag{34}$$

where the constant isentropic exponent k is equal to 1.38 and the compressor adiabatic efficiency η_a equal to 0.84.

The operating mode of the compressor for every time period is denoted by the binary variable i^a_{ts}, which is equal to 1 for open active status and 0 for closed status, in which case flows and adjacent pressures are decoupled. This configuration is expressed by the following set of equations:

$$i^a_{ts} \cdot \underline{q^a} \leq q^a_{ts} \leq i^a_{ts} \cdot \overline{q^a} \quad \forall a \in \mathcal{A}_{cm},\ t \in \mathcal{T}, s \in \mathcal{S} \tag{35}$$

$$i^a_{ts} \cdot \underline{HP^a} \leq HP^a_{ts} \leq i^a_{ts} \cdot \overline{HP^a} \quad \forall a \in \mathcal{A}_{cm},\ t \in \mathcal{T}, s \in \mathcal{S} \tag{36}$$

$$p^n_{ts} - p^m_{ts} \geq \underline{\Delta^a} \cdot i^a_{ts} + (\underline{p^n} - \overline{p^m}) \cdot (1 - i^a_{ts}) \quad \forall a = (m,n) \in \mathcal{A}_{cm}, \quad t \in \mathcal{T},\ s \in \mathcal{S} \tag{37}$$

$$p^n_{ts} - p^m_{ts} \leq \overline{\Delta^\alpha} \cdot i^a_{ts} + (\overline{p^n} - \underline{p^m}) \cdot (1 - i^a_{ts}) \quad \forall a = (m,n) \in \mathcal{A}_{cm}, t \in \mathcal{T}, s \in \mathcal{S} \tag{38}$$

$$p^n_{ts} \geq \underline{rt^a} \cdot p^m_{ts} - (1 - i^a_{ts}) \cdot (\underline{rt^a} \cdot \overline{p^m} + \underline{p^n}) \quad \forall a = (m,n) \in \mathcal{A}_{cm}, \quad t \in \mathcal{T},\ s \in \mathcal{S} \tag{39}$$

$$p^n_{ts} \leq \overline{rt^a} \cdot p^m_{ts} - (1 - i^a_{ts}) \cdot (\overline{rt^a} \cdot \underline{p^m} + \overline{p^n}) \quad \forall a = (m,n) \in \mathcal{A}_{cm}, \quad t \in \mathcal{T},\ s \in \mathcal{S} \tag{40}$$

where rt^a denotes the compressor pressure increase ratio p^n_{ts}/p^m_{ts} and

$$\underline{rt^a} \leq \frac{p^n_{ts}}{p^m_{ts}} \leq \overline{rt^a} \quad \forall a = (m,n) \in \mathcal{A}_{cm},\ t \in \mathcal{T}, s \in \mathcal{S} \tag{41}$$

Furthermore, gas flow can circumvent the compressor through by a parallel bypass valve, whose operating mode is denoted by binary ib^a_{ts} and for which condition (42) holds for every dispatch period.

$$i^a_{ts} + ib^a_{ts} = 1 \quad \forall a \in \mathcal{A}_{cm},\ t \in \mathcal{T}, s \in \mathcal{S} \tag{42}$$

Control valves represent active elements that, when active, decrease pressure along pipes $a = (m,n) \in \mathcal{A}_{cv}$ at predetermined set points at their outgoing nodes. Their operation is modelled through binary variable j^a_{ts}, denoting their status as either open when equal to 1 and closed when equal to 0. The analytical modelling of control valves is described by equations (43)-(45).

$$j^a_{ts} \cdot \underline{q^a} \leq q^a_{ts} \leq j^a_{ts} \cdot \overline{q^a} \quad \forall a \in \mathcal{A}_{cv},\ t \in \mathcal{T}, s \in \mathcal{S} \tag{43}$$

$$(\overline{p^n_{ts}} - \underline{p^m_{ts}} + \underline{\Delta^a}) \cdot j^a_{ts} + p^n_{ts} - p^m_{ts} \leq \overline{p^n_{ts}} - \underline{p^m_{ts}} \quad \forall a = (m,n) \in \mathcal{A}_{cv}, \quad t \in \mathcal{T},\ s \in \mathcal{S} \tag{44}$$

$$(\overline{p^m_{ts}} - \underline{p^n_{ts}} - \overline{\Delta^\alpha}) \cdot j^a_{ts} + p^m_{ts} - p^n_{ts} \leq \overline{p^m_{ts}} - \underline{p^n_{ts}} \quad \forall a = (m,n) \in \mathcal{A}_{cv},\ t \in \mathcal{T}, s \in \mathcal{S} \tag{45}$$

where Δ^α denotes the available pressure decrease along the control valve.

From an operation standpoint, the gas network operation is usually considered by researchers as a feasibility check problem for the stanionary case. However, since the operation of the compressor incurs actual costs, the gas problem objective C^{GAS} is selected such that all pressure, flow and active components' operational status constraints (28)-(45) are respected, while minimizing compressor costs C^{CM}_s and ensuring target non-electric demand offtakes, expresed by the penalization of their associated penalty shedding costs C^{SH}_s.

D. ELECTRICITY-GAS SYSTEMS COUPLING CONSTRAINT

The mathematical expression of the system coupling equation is formulated as:

$$u_{gts} \frac{a_g + b_g e_{gts} + c_g \left(e_{gts}\right)^2}{H} = q^m_{ts} \quad \forall g \in \mathcal{G}^{gas}, \quad m \in \mathcal{V}_e,\ t \in \mathcal{T}, s \in \mathcal{S} \tag{46}$$

Using this constraint, the electricity generation e_{gts} of thermal gas-fired units is converted to gas consumption q^m_{ts}. The

fuel consumption coefficients (a_g, b_g, c_g) of generating units' gas consumption and the higher heating value of natural gas H are used to perform the conversion. It is assumed that gas composition does not vary among the system entries and therefore no gas mixing is taken into account.

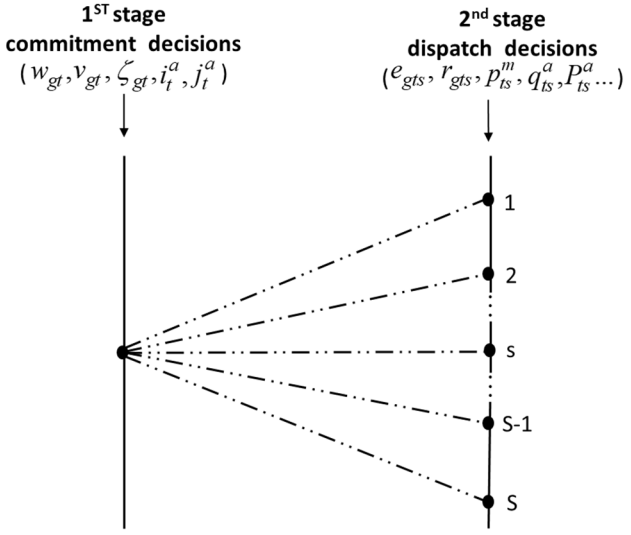

FIGURE 1. **Two-stage scenario tree.**

E. NON-ANTICIPATIVITY CONSTRAINTS

Equations (47)-(51) describe the non-anticipativity constraints of the problem. To be more specific, equations (47)-(49) denote the electricity-side constraints, enforcing the common commitment, start-up and shut-down status of lignite units and CCGTs among all examined scenarios *s,* respectively. OCGTs and hydro units' commitment decisions are allowed to be taken at intra-day dispatch horizon, therefore no such constraints are required for these units. Equation (50) on the other hand enforces the common hourly compressor operating state, which constitutes the gas side binding binary scheduling decision, while (51) selects the control valve state, respectively. Fig. 1 presents the 1st stage (here and now) and 2nd stage (wait and see) decisions of the integrated scheduling model.

$$u_{gts} = w_{gt} \quad \forall g \in \mathcal{G},\ t \in \mathcal{T}, s \in \mathcal{S} \tag{47}$$

$$y_{gts} = v_{gt} \quad \forall g \in \mathcal{G},\ t \in \mathcal{T}, s \in \mathcal{S} \tag{48}$$

$$z_{gts} = \zeta_{gt} \quad \forall g \in \mathcal{G},\ t \in \mathcal{T}, s \in \mathcal{S} \tag{49}$$

$$i_{ts}^a = h_t^a \quad \forall a \in \mathcal{A}_{cm},\ t \in \mathcal{T}, s \in \mathcal{S} \tag{50}$$

$$j_{ts}^a = \xi_t^a \quad \forall a \in \mathcal{A}_{cv},\ t \in \mathcal{T}, s \in \mathcal{S} \tag{51}$$

F. RELAXATION OF NONLINEAR EQUATIONS

Mathematical relaxation is applied to all nonlinear model equations in order to render the stochastic problem computationally tractable. Since all nonlinearities lay on the gas part of the combined model, the following discretization techniques are performed:

a) The extended incremental method is used to handle the nonlinearities in Weymouth equation (32) and in coupling equation (46). The idea is to construct piecewise MIP-relaxations of the nonlinearities in the equations with predefined errors ε_1 and ε_2, respectively, as described in more detail in the Appendix [34]. For the model described herein, the predefined errors for the extended incremental method are selected as 15 bar^2 and 1000 MW^2, for squared pressures and gas-fired power generation, respectively.
b) The coupling equation (46) is further decoupled from the unit commitment binary by applying the big M method, as analyzed in the Appendix.
c) Finally, the compressor operating range inequalities (33) are linearized via an outer approximation scheme for convex relaxations [36], which follows the mixed-integer linear reformulation procedure analytically presented in Chapter 6 of [37].

After the relaxation of all non-linear model constraints, the overall two-stage optimization problem is formulated as a Mixed Integer Linear Programming (MILP) model.

IV. ILLUSTRATIVE IMPLEMENTATIONS

A. CASE STUDY

A test case based on actual real-world conditions (typical days of January 2020) of the Greek electricity and natural gas systems is used in this section for the evaluation of the two-stage stochastic optimization approach. The examined test system comprises a total number of 28 thermal generating units and 18 hydro units; the range of energy and reserve offers per unit category is presented in Table 2.

TABLE 2. **Summary of Generation Units in the Greek Power System.**

Unit Type	Num	Capacity (MW)	Energy Offer (€/MWh)	FCR / aFRR / mFRR offer (€/MW/h)
Lignite	14	3,912	45 – 53	9.05-9.33 / No Offer / 0.01
CCGT	11	4,755	63 – 80	0.001-3.1 / 0.001-10 / 0.01
OCGT	3	147	150 - 300	10 / 10 / 10
Hydro	18	3,115	100+	No Offer / 0.001 / 0.01

The Greek gas transmission system is graphically presented in Fig. 2, where the topology of the gas-fired generating units is depicted. The Greek gas transmission system constitutes a radial tree structure comprising 3 supply entries, 34 non-electric and 11 electric gas demand nodes, along with a compressor and one control valve. The full system representation is analytically described in [38] as GasLib-134 gas network. The historical (2017-2020) gas entry distribution of the three entry nodes has been considered for the designation of the typical nominations of suppliers in the entry points, which led to 45% of the gas injections supplied through Sidirokastro, 15% supplied through Kipi and 40% supplied by Revythoussa LNG terminal. The pressure at the prevalent entry node (Sidirokastro) was set to its lower bound

FIGURE 2. **Graphical illustration of the Greek gas transmission system.**

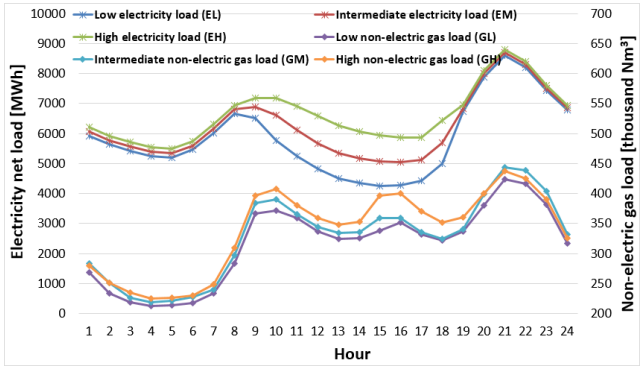

FIGURE 3. **Electricity net load and non-electric gas load scenarios.**

for every time period in order to stress the operation (technical constraints) of the gas network.

The stochastic parameters for the integrated scheduling problem constitute the electricity net load and the gas non-electric (residential, commercial, industrial) demand. Fig. 3 presents the examined three electricity net load (demand minus RES injections) scenarios stemming from a typical day-ahead forecast and considering that the RES injections forecast errors increase with the forecast lead time (as a percentage of the level of RES injections) [39]. These scenarios are hereinafter designated as EL-EM-EH. Similarly, the three gas non-electric load scenarios stem from typical hourly load profiles of winter days in Greece, expressing typical low, intermediate and high demand cases (hereinafter designated as GL-GM-GH, respectively), ranging from 7500 to 8100 thousand Nm^3 on daily basis.

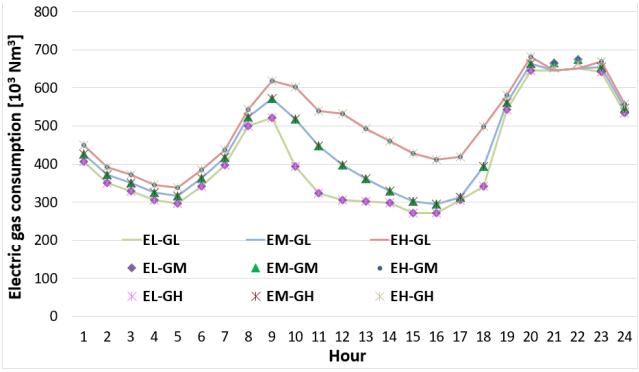

FIGURE 4. **Electric gas consumption in the nine designated scenarios.**

As a result, the cartesian product of the above electricity and gas load scenarios define nine scenarios in total to be inserted in the presented stochastic programming model with equal probabilities.

B. TEST CASE RESULTS

The results of the stochastic model are provided in this section. Fig. 4 depicts the total gas consumption of gas-fired generating units in all nine designated scenarios, which essentially reveals their production schedules during the examined days. As expected, there is a significant differentiation in the low and high electricity net load scenarios, since the CCGTs constitute intermediate load units in Greece (see Table 2), i.e. covering the intermediate load of the day, whereas their production is "shaved" in peak-load hours of 20-23 due to increased non-electric gas demand activating the gas network (i.e. lower pressure) constraints.

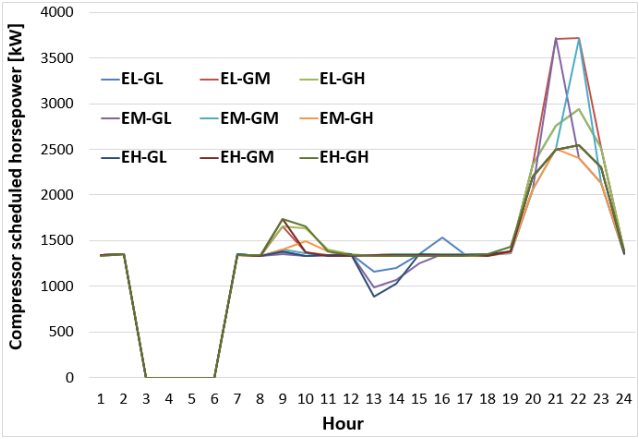

FIGURE 5. **Compressor horsepower schedule in the stochastic model solution.**

Fig. 5 illustrates the compressor scheduled horsepower for the nine scenarios as a result of the stochastic model execution. The compressor is up-and-running (binary decision) at hours 1-2 and 7-24 considering all possible real-time realizations. The illustrated day-ahead compressor horsepower

schedules are slightly differentiated due to the different conditions encountered in each scenario, but at the day-ahead horizon they represent indicative schedules; the actual dispatch shall be determined closer to real-time considering the actual realization of system conditions.

In order to evaluate the solution attained by the stochastic model, we simulate the current practice in the daily scheduling and dispatch process of the power and gas TSOs, which is to execute deterministically the day-ahead scheduling process with the base case (selected as the intermediate scenario EM-GM) and then, considering the attained commitment decisions for the generating units and the compressor, respectively, dispatch both units and the compressor[1] in real-time based on the electric and gas load realizations.

The deterministic solution of the scenario EM-GM yields the commitment decisions depicted in Fig. 6 in blue color for the generating units and for the compressor, whereas the stochastic solution respective commitment decisions are illustrated in pink color. Only the CCGTs with different commitment decisions, as compared to the stochastic model's solution, are illustrated (namely ''LAVRIO4'', MEGALOPOLI5 and ''THISVI''), shown in Fig. 6(a)(b)(c). A different commitment schedule is also derived for the compressor, as shown in Fig. 6(d), while the control valve remains open throughout the whole examined day.

Considering the commitment decisions of the stochastic model solution, all electricity net load and gas load realizations result in feasible dispatch of the resources covering the load of both systems. On the other hand, considering the commitment decisions of the deterministic model solution, both intermediate electricity and gas load realizations (EM-XX and XX-GM, respectively) do not lead to any type of infeasibilities, expressed as either RES curtailments for the electricity system or non-electric gas load shedding for the gas system. However:

a) The low net electricity load realizations (EL-XX) lead to RES curtailments at the 15th and 16th hours of the day, as shown in Fig. 6(e). This is attributed to the fact that the electricity net load reaches its daily minimum level and, even though all thermal units operate at their technical minimum, there still is electricity production surplus expressed as RES curtailments of 26 and 38 MWh during these hours, respectively. This surplus stems from the fact that in the deterministic model solution THISVI (having a technical minimum of 230 MW) is committed during hours 15 and 16, whereas in the stochastic model solution THISVI is non-committed but LAVRIO 4 (with a technical minimum of 94 MW) is taking over to cover the electricity load and the reserve requirements. The difference of 136 MW in the dispatch of the two units leads to the RES curtailment in the deterministic model solution.

b) The high gas load realizations (XX-GH) lead to non-electric gas load shedding (10886 Nm^3 in total) at the 15th and 16th hour of the day, as shown in Fig. 6(f). Even though all CCGT units are dispatched at their technical minimum in order to provide extra network capacity for the gas supplies to meet the (priority) non-electric gas demand, shedding still occurs due to the combined effect that: (a) the main supply entry (i.e. SIDIROKASTRO at the northern part of the network) is operating at minimum pressure, (b) the compressor is out of operation (see Fig. 6(d)) during these two hours, (c) the LNG source lies at the southern part of the network, and (d) the shed gas load is located at the middle of the north-south axis of the gas transmission network (in exit point ''VOLOS'' in Fig. 2). Thus, the overall gas network (i.e. pressure) constraints and the maximum injection bound of the LNG terminal to the pipeline cannot facilitate the full covering of the gas target load at node ''VOLOS''. On the other hand, in the stochastic model solution the compressor is committed as active during hours 15 and 16 (see Fig. 6(d)) and the pressure constraints for the gas flow from the northern to the southern part of the network are not activated, resulting in no gas shedding.

TABLE 3. Dispatch Cost In each Scenario Realization.

	Deterministic model			Stochastic model		
Scen. coding	Electricity cost [k€]	Gas cost [k€]	Total cost [k€]	Electricity cost [k€]	Gas cost [k€]	Total cost [k€]
EL-GL	5,915.9	2.0	5,917.9	5,912.7	2.8	5,915.5
EM-GL	6,486.3	2.0	6,488.3	6,509.5	2.9	6,512.4
EH-GL	7,470.5	2.0	7,472.5	7,249.1	2.9	7,252.0
EL-GM	5,934.1	2.4	5,936.5	5,930.2	3.0	5,933.1
EM-GM	6,517.4	2.1	6,519.5	6,526.7	3.0	6,529.7
EH-GM	7,556.2	2.1	7,558.3	7,266.6	3.0	7,269.7
EL-GH	5,926.6	14.9	5,941.5	5,920.0	2.8	5,922.8
EM-GH	6,511.1	14.6	6,525.7	6,516.7	2.9	6,519.6
EH-GH	7,557.9	14.2	7,572.2	7,256.4	3.0	7,259.3

The overall dispatch cost in each of the nine realizations in both the deterministic and stochastic models' solutions is presented in Table 3, considering a penalty cost equal to 150 €/MWh for RES curtailments and equal to 1.725 €/Nm^3 for the shed gas quantities. As shown, in all realizations except from EM-GM (base case, which was used as input for the deterministic model solution) and EM-GL the stochastic model outperforms the deterministic model in terms of overall system cost. The cost differences range from 220-313 k€ in realizations EH-XX where the maximum savings are attained, 2-19 k€ in realizations EL-XX, and about 6 k€ in realization EM-GH. As noted above, in realizations EM-GL and EM-GM the deterministic model solution

[1]In practice, most gas TSOs do not even dispatch on hourly basis the compressor in real-time but decide its dispatch level in day-ahead and operate the compressor at this level without any intra-day dispatch fluctuations. However, for the sake of the comparison with the stochastic case and in order to be more fair with the deterministic approach, we consider that the gas TSOs act in a vigilant way and change the compressor horsepower when needed to constantly regulate the nodal pressures and optimize the gas transmission system operation in terms of compressor cost savings. In addition, compressor horsepower exhibits hourly ramping constraints in real operation, which were omitted in the current model to alleviate the computational burden.

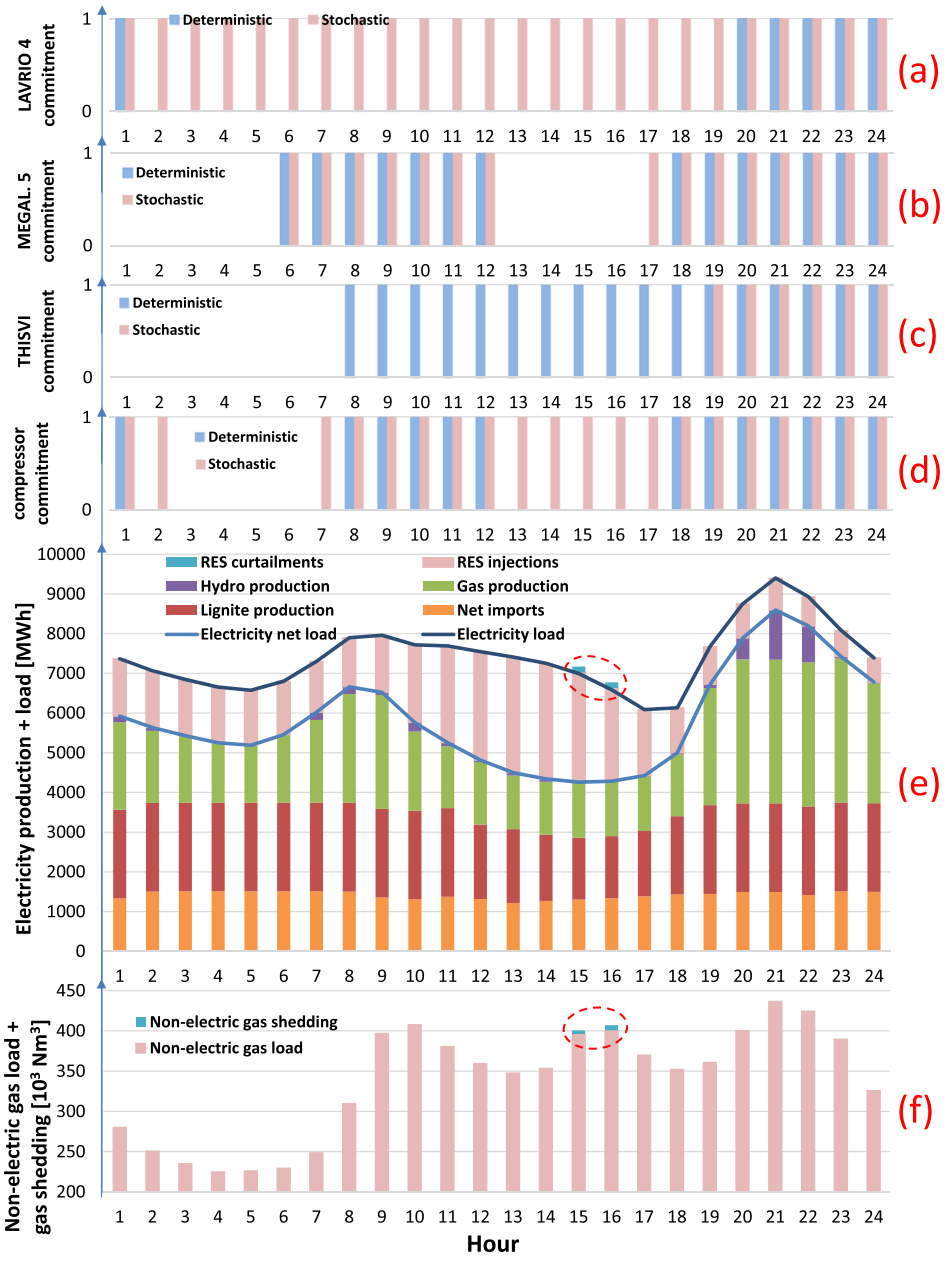

FIGURE 6. **Deterministic vs. stochastic solution results.**

is better than the stochastic one by about 24 and 10 k€, respectively. Considering the probabilities of the stochastic scenarios, the average savings encountered by use of the stochastic model amounts to about 91 k€.

C. COMPUTATIONAL ASPECTS

The proposed optimization model was solved in a desktop PC equipped with an i7/8-Core/4.0 GHz CPU processor and 16 GB of RAM, using the GAMS modeling software [41] and the Gurobi 9.0 solver with a MIP optimality gap tolerance 0.1% [42]. The implemented linearized gas model was built with the C++ software LaMaTTo++ [43]. The problem comprises 511,723 constraints with 37,896 binary and 359,659 continuous variables. The overall computational time for the examined 9 scenarios is about 20 minutes, which is considered acceptable for the current industry standards.

The selection of error ε in the extended incremental method plays an important role in the execution of the integrated model. The smaller the error selected, the closer the relaxed problem's solution would be to the respective master MINLP, to the detriment of model size and complexity since a very tight relaxation leads to increased number of continuous and binary variables. This would make it impossible to solve the problem within reasonable execution times. On the other hand, a large selected error would result in short execution times, albeit with random solutions that would have

no practical meaning for the examined problem. In order to examine the effect of changing the error bounds, a sensitivity analysis is performed in this section. For the integrated model presented in this paper, the decrease in the error bound for the squared pressures ε_1 from 15 bar^2 to 10, 5 or 1 bar^2 makes the model intractable, regardless of the selected error for the squared power outputs. For this reason, ε_1 is kept constant and a sensitivity analysis with the error bound for the squared power outputs ε_2 was performed; the results in terms of number of equations and variables as well of execution times are presented in Table 4. As shown, the only value of ε_2 that yields a solution time less than one hour (which was set as the solution time maximum limit) is 1000 MW^2. All other selections result in higher accuracy but also to higher solution times.

TABLE 4. Solution Performance Indices.

max error (MW^2)	Number of equations	Number of continuous variables	Number of binary variables	Solution time (sec)
5	837,235	468,307	146,760	23,837
10	780,211	449,515	127,752	5,274
50	616,267	394,867	73,104	4,918
100	575,443	381,259	59,496	3,712
1000	511,723	359,659	37,896	1,220

V. CONCLUSION AND FURTHER RESEARCH

This paper presents a stochastic two-stage formulation for the integrated solution of the electricity and gas systems with uncertainty on both the electricity and the gas side, that incorporates (a) the full unit-commitment modeling for the explicit modeling of the electricity power system and (b) a detailed configuration of the gas network incorporating linearized gas network constraints. Three distinct linearization techniques (extended incremental method, outer approximation and big M method) for the linearization of the Weymouth equation, the compressor operating range and the electricity-gas coupling equation, respectively, were incorporated in a stochastic model for the integrated solution of the two systems. The use of the binary/discrete decisions for the operating control components of the gas network (i.e. the compressor commitment) provides extra control to the gas TSO at the scheduling stage.

The stochastic model has been evaluated in a medium-size real-world test system considering nine electricity net load and gas load scenarios. The test results prove that the presented stochastic model solution outperforms the respective deterministic one (which constitutes the current best practice of electricity and gas TSOs), since it leads to zero infeasibilities and curtailments (i.e. RES curtailments and/or non-electric gas load shedding) in real-time. The stochastic model was solved one-shot using a commercial solver in acceptable time limits.

Further research shall be targeted at handling more electricity and gas scenarios and at the implementation of adequate decomposition techniques for (a) the solution of the underlying optimization problem in shorter execution times and (b) to accommodate tighter mixed-integer relaxations.

APPENDIX

The extended incremental method is adopted for the linearization of the nonlinearities that arise in the gas subproblem due to its better performance compared to other linearization methods [40] and its well-examined application in large-scale gas networks [37]. The target is to construct MIP approximations of a univariate nonlinear function $f(y)$ that satisfy a predefined upper bound ε for nonlinearity violations.

To this end, a piecewize linear interpolation $\varphi(y)$ of f is constructed over a finetely bounded interval $[\underline{y}, \bar{y}]$, such that the approximation error bound ε is satisfied, i.e. $\max_y |f(y) - \varphi(y)| \leq \varepsilon$, as proposed in [32]. The $\varphi(y)$ function is expressed as the piecewise interpolation of *n-1* breakpoints $b \in [b_o = y_{\min}, b_n = y_{\max}]$ defined over n segments, and the extended incremental method is applied after the substitution of $z = \varphi(y)$ by the following system:

$$y = b_o + \sum_{i=1}^{n} (b_i - b_{i-1})\delta_i \tag{52a}$$

$$z = f(b_o) + \sum_{i=1}^{n} (f(b_i) - f(b_{i-1}))\delta_i + \tau \tag{52b}$$

$$\delta_{i+1} \leq w_i \leq \delta_i \quad \forall i = 1, \ldots, n-1 \tag{52c}$$

$$0 \leq \delta_i \leq 1 \quad \forall i = 1, \ldots, n \tag{52d}$$

$$w_i \in \{0, 1\} \quad \forall i = 1, \ldots, n-1 \tag{52e}$$

Each of the δ variables is associated with a discretization interval n and due to the filling condition (52c) $0 \leq \delta_n \leq w_{n-1} \leq \delta_{n-1} \leq \ldots \leq w_1 \leq \delta_1 \leq 1$, we ensure that every feasible point of the above system $\delta_i \geq 0$ requires $\delta_j = w_j = 1$ for all $j \leq i$ and that $\delta_i \leq 1$ requires $\delta_j = w_j = 0$ for all $j \geq i$. This way, there can only be at most one active index i of an interval with $0 < \delta_i < 1$ with all preceding intervals j at $\delta_j = 1$.

With the addition of the variable τ in (52b) $\tau \in [-\varepsilon, \varepsilon]$, all points (y,z) lay within a box of *2t* height that encloses the graph of the piecewise linear function, ensuring that $|f(y^*) - z^*| \leq \varepsilon$ holds for all feasible points that satisfy (52). We again refer to [34] and [35] for more details on the method.

The extended incremental method is applied for the given model equations in the form of nonlinear functions $f(y) = y^2$ which, in the case of the integrated power-gas problem, are expressed by $(y, z) = \{(p_m, \pi_m), (p_n, \pi_m), (\omega_g, e_g)\}$, where $p_m^2 = \pi_m$, $p_n^2 = \pi_n$ and $e_g^2 = \omega_g$. All equations of the system are indexed by time $t \in \mathcal{T}$ and scenario $s \in \mathcal{S}$ sets, though not displayed here for simplicity purposes.

To futher decouple the binary variables u_g from the power generation variables e_g in coupling equation (46), after the discretization of the squared power generation, the big M method is applied as follows:

$$\delta_{ig} \leq u_g \tag{53a}$$

$$\psi_g = \frac{a_g + b_g e_g + c_g \omega_g}{H} \tag{53b}$$

$$\varphi_g \geq \psi_g - (1 - u_g)M \tag{53c}$$

$$\varphi_g \leq \psi_g + (1 - u_g)M \tag{53d}$$
$$\varphi_g \leq u_g M \tag{53e}$$
$$\varphi_g \leq \psi_g \tag{53f}$$

where φ_g and ψ_g auxiliary positive variables and $e_g^2 = \omega_g$. Parameter M is taken equal to $\left(a_g + b_g e_g^{max} + c_g \left(e_g^{max}\right)^2\right)/H$, with e_g^{max} being the highest maximum available capacity of all gas-fired units $g \in \mathcal{G}^{gas}$.

ACKNOWLEDGMENT

The authors would like to thank Björn Geißler and Mathias Sirvent for their assistance in setting up the gas scenarios in LaMaTTo++ and their insights on the mathematical implementation of the integrated model.

REFERENCES

[1] ENTSO-E. (Nov. 2019). *The Gas and Electricity ENTSOs Publish Their Joint Scenarios for TYNDP 2020*. [Online]. Available: https://www.entsoe.eu/news/2019/11/12/the-gas-and-electricity-entsos-publish-their-joint-scenarios-for-tyndp-2020/

[2] (Jul. 2019). *Joint Institute for Strategic Energy Analysis, Managing the Electricity-Gas Interface: Current Environment and Emerging Solutions*. [Online]. Available: https://www.nrel.gov/docs/fy19osti/71750.pdf

[3] M. Shahidehpour and Z. Li, "Long-term electric and natural gas infrastructure requirements," Illinois Inst. Technol., Chicago, IL, USA, White Paper, Nov. 2014. [Online]. Available: https://pubs.naruc.org/pub/536DCA2E-2354-D714-5112-CBD58ED9B81A

[4] A. Zlotnik, L. Roald, S. Backhaus, M. Chertkov, and G. Andersson, "Coordinated scheduling for interdependent electric power and natural gas infrastructures," *IEEE Trans. Power Syst.*, vol. 32, no. 1, pp. 600–610, Jan. 2017.

[5] C. He, T. Liu, L. Wu, and M. Shahidehpour, "Robust coordination of interdependent electricity and natural gas systems in day-ahead scheduling for facilitating volatile renewable generations via power-to-gas technology," *J. Mod. Power Syst. Clean Energy*, vol. 5, no. 3, pp. 375–388, Apr. 2017.

[6] C. Liu, M. Shahidehpour, and J. Wang, "Application of augmented Lagrangian relaxation to coordinated scheduling of interdependent hydrothermal power and natural gas systems," *IET Gener., Transmiss. Distrib.*, vol. 4, no. 12, pp. 1314–1325, Dec. 2010.

[7] B. Zhao, A. Zlotnik, A. J. Conejo, R. Sioshansi, and A. M. Rudkevich, "Shadow price-based co-ordination of natural gas and electric power systems," *IEEE Trans. Power Syst.*, vol. 34, no. 3, pp. 1942–1954, May 2019.

[8] G. Byeon and P. Van Hentenryck, "Unit commitment with gas network awareness," *IEEE Trans. Power Syst.*, vol. 35, no. 2, pp. 1327–1339, Mar. 2020.

[9] C. M. Correa-Posada and P. Sanchez-Martin, "Integrated power and natural gas model for energy adequacy in short-term operation," *IEEE Trans. Power Syst.*, vol. 30, no. 6, pp. 3347–3355, Nov. 2015.

[10] C. M. Correa-Posada, P. Sánchez-Martìn, and S. Lumbreras, "Security-constrained model for integrated power and natural-gas system," *J. Modern Power Syst. Clean Energy*, vol. 5, no. 3, pp. 326–336, Apr. 2017.

[11] S. Clegg and P. Mancarella, "Integrated modeling and assessment of the operational impact of power-to-gas (P2G) on electrical and gas transmission networks," *IEEE Trans. Sustain. Energy*, vol. 6, no. 4, pp. 1234–1244, Oct. 2015.

[12] L. Bai, F. Li, H. Cui, T. Jiang, H. Sun, and J. Zhu, "Interval optimization based operating strategy for gas-electricity integrated energy systems considering demand response and wind uncertainty," *Appl. Energy*, vol. 167, pp. 270–279, Apr. 2016.

[13] T. Ding, Y. Xu, W. Wei, and L. Wu, "Energy flow optimization for integrated power–gas generation and transmission systems," *IEEE Trans.Ind. Inform.*, vol. 16, no. 3, pp. 1677–1687, Mar. 2020.

[14] S. Chen, A. J. Conejo, R. Sioshansi, and Z. Wei, "Unit commitment with an enhanced natural gas-flow model," *IEEE Trans. Power Syst.*, vol. 34, no. 5, pp. 3729–3738, Sep. 2019.

[15] C. He, X. Zhang, T. Liu, L. Wu, and M. Shahidehpour, "Coordination of interdependent electricity grid and natural gas network—A review," *Current Sustain./Renew. Energy Rep.*, vol. 5, pp. 23–36, Feb. 2018.

[16] Q. P. Zheng, J. Wang, and A. L. Liu, "Stochastic optimization for unit commitment—A review," *IEEE Trans. Power Syst.*, vol. 30, no. 4, pp. 1913–1924, Jul. 2015.

[17] C. M. Correa-Posada and P. Sanchez-Martin, "Stochastic contingency analysis for the unit commitment with natural gas constraints," in *Proc. IEEE Grenoble Conf.*, Grenoble, France, Jun. 2013, pp. 16–20.

[18] A. Antenucci and G. Sansavini, "Stochastic unit commitment and reserve scheduling under gas-supply disrupted scenarios," in *Proc. IEEE Int. Energy Conf. (ENERGYCON)*, Jun. 2018, pp. 1–6.

[19] M. Qadrdan, J. Wu, N. Jenkins, and J. Ekanayake, "Operating strategies for a GB integrated gas and electricity network considering the uncertainty in wind power forecasts," *IEEE Trans. Sustain. Energy*, vol. 5, no. 1, pp. 128–138, Jan. 2014.

[20] M. A. Mirzaei, A. S. Yazdankhah, B. Mohammadi-Ivatloo, M. Marzband, M. Shafie-khah, and J. P. S. Catalão, "Stochastic network-constrained co-optimization of energy and reserve products in renewable energy integrated power and gas networks with energy storage system," *J. Cleaner Prod.*, vol. 223, pp. 747–758, Jun. 2019.

[21] D. Hu and S. M. Ryan, "Stochastic vs. deterministic scheduling of a combined natural gas and power system with uncertain wind energy," *Int. J. Elect. Power Energy Syst.*, vol. 108, pp. 303–313, Jun. 2019.

[22] A. Alabdulwahab, A. Abusorrah, X. Zhang, and M. Shahidehpour, "Stochastic security-constrained scheduling of coordinated electricity and natural gas infrastructures," *IEEE Syst. J.*, vol. 11, no. 3, pp. 1674–1683, Sep. 2017.

[23] Y. Li *et al.*, "Optimal stochastic operation of integrated low-carbon electric power, natural gas, and heat delivery system," *IEEE Trans. Sustain. Energy*, vol. 9, no. 1, pp. 273–283, Jan. 2018.

[24] B. Zhao, A. J. Conejo, and R. Sioshansi, "Unit commitment under gas-supply uncertainty and gas-price variability," *IEEE Trans. Power Syst.*, vol. 32, no. 3, pp. 2394–2405, May 2017.

[25] Y. Xu, T. Ding, M. Qu, and P. Du, "Adaptive dynamic programming for gas-power network constrained unit commitment to accommodate renewable energy with combined-cycle units," *IEEE Trans. Sustain. Energy*, vol. 11, no. 3, pp. 2028–2039, Jul. 2020.

[26] L. Bai, F. Li, T. Jiang, and H. Jia, "Robust scheduling for wind integrated energy systems considering gas pipeline and power transmission N–1 contingencies," *IEEE Trans. Power Syst.*, vol. 32, no. 2, pp. 1582–1584, Mar. 2017.

[27] C. He, L. Yu, T. Liu, and Z. Bie, "Robust co-optimization planning of interdependent electricity and natural gas wystems with a joint N-1 and probabilistic reliability criterion," *IEEE Trans.Power Syst.*, vol. 33, no. 2, pp. 2140–2154, Mar. 2018.

[28] Y. He, M. Shahidehpour, Z. Li, C. Guo, and B. Zhu, "Robust constrained operation of integrated electricity-natural gas system considering distributed natural gas storage," *IEEE Trans. Sustain. Energy*, vol. 9, no. 3, pp. 1061–1071, Jul. 2018.

[29] S. Chen, Z. Wei, G. Sun, K. W. Cheung, D. Wang, and H. Zang, "Adaptive robust day-ahead dispatch for urban energy systems," *IEEE Trans. Ind. Electron.*, vol. 66, no. 2, pp. 1379–1390, Feb. 2019.

[30] F. Liu, Z. Bie, and X. Wang, "Day-ahead dispatch of integrated electricity and natural gas system considering reserve scheduling and renewable uncertainties," *IEEE Trans. Sustain. Energy*, vol. 10, no. 2, pp. 646–658, Apr. 2019.

[31] C. He, X. Zhang, T. Liu, C. Guo, and L. Wu, "Distributionally robust scheduling of integrated gas-electricity systems with demand response," *IEEE Trans. Power Syst.*, vol. 34, no. 5, pp. 3791–3803, Sep. 2019.

[32] Y. Zhang, J. Le, F. Zheng, Y. Zhang, and K. Liu, "Two-stage distributionally robust coordinated scheduling for gas-electricity integrated energy system considering wind power uncertainty and reserve capacity configuration," *Renew. Energy*, vol. 135, pp. 122–135, May 2019.

[33] M. Sirvent, N. Kanelakis, B. Geißler, and P. Biskas, "Linearized model for optimization of coupled electricity and natural gas systems," *J. Modern Power Syst. Clean Energy*, vol. 5, no. 3, pp. 364–374, May 2017.

[34] B. A. Geißler Martin and A. L. Morsi Schewe, "Using piecewise linear functions for solving MINLPs," in *Mixed Integer Nonlinear Programming*. (The IMA Volumes in Mathematics and its Applications), vol. 154, J. Lee and S. Leyffer, Eds. New York, NY, USA: Springer, 2012.

[35] B. Geißler, "Towards globally optimal solutions for MINLPs by discretization techniques with applications in gas network optimization," Ph.D. dissertation, Dept. EDOM, Math., Univ. Erlangen-Nuremberg, Erlangen, Germany, 2011.

[36] M. A. Duran and I. E. Grossmann, "An outer-approximation algorithm for a class of mixed-integer nonlinear programs," *Math. Program.*, vol. 36, no. 3, pp. 307–339, Oct. 1986.
[37] T. Koch *et al.*, *Evaluating Gas Network Capacities* (MOS-SIAM Series on Optimization). Philadelphia, PA, USA: SIAM, 2015.
[38] M. Schmidt *et al.*, "GasLib—A library of gas network instances," *Data*, vol. 2, no. 4, p. 40, Dec. 2017.
[39] E. A. Bakirtzis, P. N. Biskas, and A. G. Bakirtzis, "The impact of load-following reserve requirement levels on the short-term generation scheduling," in *Proc. Power Syst. Comput. Conf. (PSCC)*, Jun. 2016, pp. 1–7.
[40] C. M. Correa-Posada and P. Sanchez-Martin. *Gas Network Optimization: A Comparison of Piecewise Linear Models*. Accessed: Jan. 10, 2020. [Online]. Available: http://www.optimization-online.org/DB_FILE/2014/10/4580.pdf
[41] *General Algebraic Modeling System*. Accessed: Feb. 12, 2020. [Online]. Available: http://www.gams.com/
[42] *Gurobi 9.0: Gurobi Optimizer Reference Manual*. Accessed: Feb. 12, 2020. [Online]. Available: http://www.gurobi.com
[43] LaMaTTo++. (2015). *A Framework for Modeling and Solving Mixed-Integer Nonlinear Programming Problems on networks*. [Online]. Available: https://en.www.math.fau.de/edom/projects-edom/mixed-integer-programming/lamatto

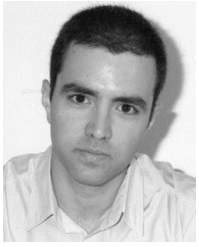

NIKOLAOS G. KANELAKIS (Graduate Student Member, IEEE) received the Dipl.-Eng. degree from the Department of Electrical and Computer Engineering, Aristotle University of Thessaloniki, Greece, where he is currently pursuing the Ph.D. degree. His research interests include power system analysis, optimization and economics, and in the integration and operation of power and natural gas systems.

PANDELIS N. BISKAS (Senior Member, IEEE) received the Dipl.-Eng. and Ph.D. degrees from the Department of Electrical and Computer Engineering, Aristotle University of Thessaloniki, Greece, in 1999 and 2003, respectively. He also performed his Postdoctoral Research at the Aristotle University of Thessaloniki from March 2004 till August 2005. From March 2005 until July 2009, he was a Power System Specialist with the Hellenic TSO, Market Operation Department. He is currently an Associate Professor with the Department of Electrical and Computer Engineering, Aristotle University of Thessaloniki. His research interests include power system operation and control, electricity market operational and regulatory issues, and transmission pricing.

DIMITRIS I. CHATZIGIANNIS (Member, IEEE) received the Dipl.Ing. and Ph.D. degrees from the Department of Electrical and Computer Engineering, Aristotle University of Thessaloniki, Greece, in 2009 and 2014, respectively. He currently works as a Senior Energy Analyst with Heron II Viotias S.A., a Greek energy utility, being responsible for the development of optimization tools for the company's electricity- and gas-related activities. His research interests include the wide area of energy economics, optimization research, and data analytics.

ANASTASIOS G. BAKIRTZIS (Fellow, IEEE) received the Dipl.Eng. degree from the Department of Electrical Engineering, National Technical University, Athens, Greece, in 1979, and the M.S.E.E. and Ph.D. degrees from the Georgia Institute of Technology, Atlanta, in 1981 and 1984, respectively.

Since 1986, he has been with the Electrical Engineering Department, Aristotle University of Thessaloniki, Greece, where he is currently a Professor. His research interests include power system operation, planning, and economics.